Gene Expression Patterns 37 (2020) 119126

Contents lists available at ScienceDirect

Gene Expression Patterns

journal homepage: www.elsevier.com/locate/gep

Expression patterns of activating transcription factor 5 (*atf5a* and *atf5b*) in zebrafish

Roberto Rodríguez-Morales [a], Viveca Vélez-Negrón [a], Aranza Torrado-Tapias [a], Gaurav Varshney [b], Martine Behra [a,*]

[a] Department of Anatomy and Neurobiology, University of Puerto Rico, Medical Sciences Campus (UPR-MSC), San Juan, PR, USA
[b] Oklahoma Medical Research Foundation (OMRF), Oklahoma City, OK, USA

ARTICLE INFO

Keywords:
Zebrafish
Activating transcription factor
Lateral line
Olfactory organ
Neuroprogenitors
Inner ear

ABSTRACT

The Activating Transcription Factor 5 (ATF5) is a basic leucine-zipper (bZIP) transcription factor (TF) with proposed stress-protective, anti-apoptotic and oncogenic roles which were all established in cell systems. In whole animals, Atf5 function seems highly context dependent. *Atf5* is strongly expressed in the rodent nose and mice knockout (KO) pups have defective olfactory sensory neurons (OSNs), smaller olfactory bulbs (OB), while adults are smell deficient. It was therefore proposed that Atf5 plays an important role in maturation and maintenance of OSNs. *Atf5* expression was also described in murine liver and bones where it appears to promote differentiation of progenitor cells. By contrast in the rodent brain, *Atf5* was first described as uniquely expressed in neuroprogenitors and thus, proposed to drive their proliferation and inhibit their differentiation. However, it was later also found in mature neurons stressing the need for additional work in whole animals. *ATF5* is well conserved with two paralogs, a*tf5a* and *atf5b* in zebrafish. Here, we present the expression patterns for both from 6 h (hpf) to 5day post-fertilization (dpf). We found early expression for both genes, and from 1dpf onwards overlapping expression patterns in the inner ear and the developing liver. In the brain, at 24hpf both *atf5a* and *atf5b* were expressed in the forebrain, midbrain, and hindbrain. However, from 2dpf and onwards we only detected *atf5a* expression namely in the olfactory bulbs, the mesencephalon, and the metencephalon. We further evidenced additional differential expression for *atf5a* in the sensory neurons of the olfactory organs, and for *atf5b* in the neuromasts, that form the superficial sensory organ called the lateral line (LL). Our results establish the basis for future functional analyses in this lower vertebrate.

1. Introduction

ATF5 was first identified as a novel ATF4-related protein (Nishizawa and Nagata, 1992) that belongs to the activating transcription factor (ATF)/cAMP response-element binding protein (CREB) family, which are basic valine-leucine zipper (bZIP) transcription factors (TFs) (Hai and Hartman, 2001) that bind DNA in homo and heterodimers (Vinson et al., 2002). Apoptosis induced by growth factor deprivation (Persengiev et al., 2002) (Persengiev and Green, 2003) or heat shock (Wang et al., 2007) demonstrated a pro-survival activity for ATF5 in some cell types. The anti-apoptotic role was also described in various tumors (for review (Sears and Angelastro, 2017)) notably in neural tumors like gliomas (Greene et al., 2009). However, numerous cell lines when stressed survive fine without ATF5 and many tumors do not express it, underlining the importance of the cellular context. Furthermore, the stability of the *ATF5* gene products seems highly context-dependent (for review (Sears and Angelastro, 2017)), and the protein can both work as an activator (Wang et al., 2007) or a repressor of target genes (Al Sarraj et al., 2005). It was also described as a promiscuous TF which can dimerize with a plethora of partners (Vinson et al., 2002) which are all likely to ultimately alter the function. The tissue-specific distribution of the dimerization partners is still poorly known and the *Atf5* expression data itself which was mostly documented in rodents, is not always concordant (Hansen et al., 2002; Angelastro et al., 2003; Arias et al., 2012; Lee et al., 2012; Mason et al., 2005; Torres-Peraza et al., 2013).

Atf5 expression was first described in developing olfactory sensory neurons (OSNs) in both rodent olfactory organs, namely the olfactory cavity and the vomeronasal organ (Hansen et al., 2002), the latter being absent in Fish and vestigial in higher primates (Sato et al., 2005; Saraiva et al., 2015). Embryonic *Atf5*-KO mice have poorly differentiated OSNs

* Corresponding author.
E-mail address: martinebehra@upr.edu (M. Behra).

https://doi.org/10.1016/j.gep.2020.119126
Received 17 December 2019; Received in revised form 7 July 2020; Accepted 7 July 2020
Available online 11 July 2020
1567-133X/

which are apoptotic in both the olfactory (OE) (Wang et al., 2012) and the vomeronasal epithelia (VNE) (Nakano et al., 2016), arguing that Atf5 is necessary for maturation and maintenance of differentiated OSNs. Post-natal homozygote animals also have smaller olfactory bulbs (OB) with less interneurons even if those cells do not express *Atf5*. This was arguably due to defective proliferation of neuroprogenitors in the sub ventricular zone (SVZ) of the telencephalon, which in adults remains neurogenic in its ventral part (Umemura et al., 2015). Furthermore, strong *Atf5* expression was found in neuroprogenitors in the ventricular zone (VZ) of the telencephalic lateral ventricle of prenatal rats, as well as in the SVZ of postnatal animals (Angelastro et al., 2003, 2005; Mason et al., 2005), where it was proposed to promote proliferation and inhibit differentiation. Two lines of evidence reinforce this hypothesis. First, in the murine prenatal cerebellum, Atf5 protein was found in proliferating cerebellar granule neuron progenitor cells (CGNPs) located in the germinal layers (Rhombic lip (RL), external granular layer (EGL) and VZ of the fourth ventricle), as well as in the EGL of postnatal animals (Lee et al., 2012). Second, in post-natal and adult mice the Atf5 protein was found in various brain regions that remain neurogenic, namely in the ependymal zone (EZ), the SVZ, the corpus callosum (CC) and the hippocampal dentate gyrus subgranular zone (Arias et al., 2012). However, a more recent systematic expression analysis which was specifically focusing on developing and adult murine brains showed that *Atf5* gene products were also abundantly expressed in post-mitotic neurons (Torres-Peraza et al., 2013), which is in line with anxiety-like behaviors described in adult *Atf5*-KOs (Umemura et al., 2017). Thus, even in the neural context where it was the best documented, Atf5 exact role remains unresolved.

Atf5 expression is also found in other embryonic and adult tissues. It is abundantly expressed in the adult mouse liver (Hansen et al., 2002) in which it was shown to be necessary for hepatocyte differentiation (Pascual et al., 2008). Fibroblasts (Nakamori et al., 2017), and induced pluripotent stem cells (Nakamori et al., 2016) that are differentiating into hepatocytes, strongly up-regulate *Atf5* expression. Likewise, in the mouse limb bud differentiating chondrocytes transiently express *Atf5* (Shinomura et al., 2006), and ES cells differentiating into embryoid bodies increase *Atf5* levels (Sampath et al., 2008). Taken together, *Atf5* appears to induce differentiation and prevent proliferation of those various progenitor cells, thus underlining the need for additional work in the physiological context of whole animals.

We propose to use embryos and larvae of the zebrafish genetic tractable vertebrate animal model. Because of a whole genome duplication that occurred in teleost Fish (Glasauer and Neuhauss, 2014), *atf5* has two highly identical paralogous genes which were named *atf5a* and *atf5b*, for which the respective expression patterns need to be resolved.

To elucidate the spatiotemporal expression pattern of both genes, we performed whole-mount *in-situ* hybridization (WISH) in 6 h post fertilization (hpf) embryos to 5day post fertilization (dpf) larvae. At 6hpf, we found weak but ubiquitous expression for both genes, which was more robust for *atf5a*. At 24hpf, we evidenced overlapping brain expression of both genes in the tectum of the midbrain, at the midbrain-hindbrain boundary and in the hindbrain. We saw segregated expression of *atf5a* in the olfactory bulbs of the forebrain, and of *atf5b* in the most rostral part of the telencephalon. At 2dpf and onwards, we only found *atf5a* expression in the brain, which was restricted to the olfactory bulbs, the mesencephalic *tectum* and the metencephalic *medulla oblongata*. Notably, all of these regions are known neurogenic centers in adult Fish (Kermen et al., 2013) (Kaslin et al., 2008). Also starting at 24hpf, both genes were expressed in the developing otic placodes and the liver primordium, and at later stages strongly expressed in the inner ear cristae and maculae, as well as in the developing liver. Furthermore, from 2dpf onwards we found exclusive expression of *atf5a* in the sensory neurons (OSNs) of the olfactory organs, and of *atf5b* in the neuromasts (NMs) of the fish specific superficial sensory organ which is called the lateral line (LL). Our work is setting the foundation that will allow dissecting ATF5 tissue specific function in a lower vertebrate animal.

2. Results

2.1. 1: atf5a and atf5b are highly identical paralogs

Using online resources (Ensembl: http://useast.ensembl.org/Danio_rerio/Info/Index; NCBI-Blast: https://blast.ncbi.nlm.nih.gov/Blast.cgi; genecards: https://www.genecards.org/cgi-bin/carddisp.pl?gene%20=%20ATF5; OMIM: https://www.omim.org/entry/606398?search=atf5&highlight=atf5), we gathered some of the available information for both paralogs, which were encoded by two separate genes. The *atf5a* gene mapped to chromosome 5 (absolute coordinates: 30,414,163–30,418,723 base pairs, bp) and was a relatively small gene (4560bp), while *atf5b* mapped to chromosome 15 (absolute coordinates 17,862,207–17,870,090 bp) and was slightly bigger (7883bp). Both genes comprised four partially translated exons which resulted in a single transcript (4390 bp long) for *atf5a* and 3 different transcripts (6910, 4030 and 579 bp long) for *atf5b* (predicted from Ensembl Genome Browser). The predicted translated proteins were for atf5a 511 amino acid (aa) long, and for the longest transcript of atf5b, 435aa long.

To analyze the degree of identity of the two paralogs we first performed a nucleotide alignment (with NCBI Blastn) with the founder gene of the *ATF4* family, *atf4*, that was also duplicated in the zebrafish genome (*atf4a* and *atf4b)*. Although *atf4b* is still very poorly described, all 4 genes can be considered paralogs, so we extended the sequence comparison to all four genes (Fig. 1A). First, we aligned the nucleotide sequences (left panel) and found poor overall identity (~83% but for only 2% of the query cover). Next, we aligned the protein sequences (with NCBI Blastp, right panel) which yielded better overall identity (~53% for 20% of the query cover) mainly restricted to the Cterm corresponding to the signature domain of the ATF4 family, the bZIP domain. Notably, the shorter 111aa long protein encoded by *atf5b* lacked the bZIP domain (not shown). When considering only atf5a and atf5b, the degree of identity (45.86%) was for a much bigger query coverage (~83%) that yielded an alignment score above 200 for the entire atf5b sequence, which was only lacking the first ~50aa forming the Nterm of atf5a. Taken together, this was suggesting that *atf4a* and *atf4b* were more divergent from both *atf5a* and *atf5b*, and putatively less likely to have overlapping functions and thus, we restricted all further analysis to *atf5a* and *atf5b* only. To address interspecies conservation, we next aligned the amino acid (aa) sequences (with NCBI Blastp) of the two zebrafish paralogs with mouse Atf5 and human ATF5 (Fig. 1B). Unsurprisingly, only the Cterm had an alignment score close to 200. The other notable region of alignment was in the proximal Nterm where the alignment score was ranging from 40 to 80, suggesting the presence of an additional functionally important region.

Next, we searched the databases (using (Nishizawa and Nagata, 1992) SWISS-MODEL, https://swissmodel.expasy.org/and (Hai and Hartman, 2001) PHYRE2, http://www.sbg.bio.ic.ac.uk/phyre2/html/page.cgi?id=index) for predicted 3D structures in atf5a and atf5b to find additional signature domains to the Cterm signature bZIP domain (Fig. 1C). As expected, the central part of the proteins which was poorly conserved across species corresponded to long stretches of low conformation (~87.5% in atf5a and 85.3% in atf5b). Nevertheless, in the most N-term region of both paralogs we found a mitochondrial targeting sequence (MTS) (Fukasawa et al., 2015), which had been previously described in ATF5 and implicated in the mitochondrial stress response (Fiorese et al., 2016). We also found in the more distal N-term of both proteins, a conserved nuclear export sequence (NES) (la Cour et al., 2004), as well as a nuclear localization signal (NLS) inside the C-term bZIP domain (Nguyen et al., 2009), suggesting a putative cytoplasmic role for atf5a and atf5b in addition to the TF function.

2.2. 2: atf5a and atf5b expression in the embryo (6–24hpf)

We synthetized sense and antisense probes against both *atf5a* and *atf5b* longest transcripts to perform wholemount *in situ* hybridizations

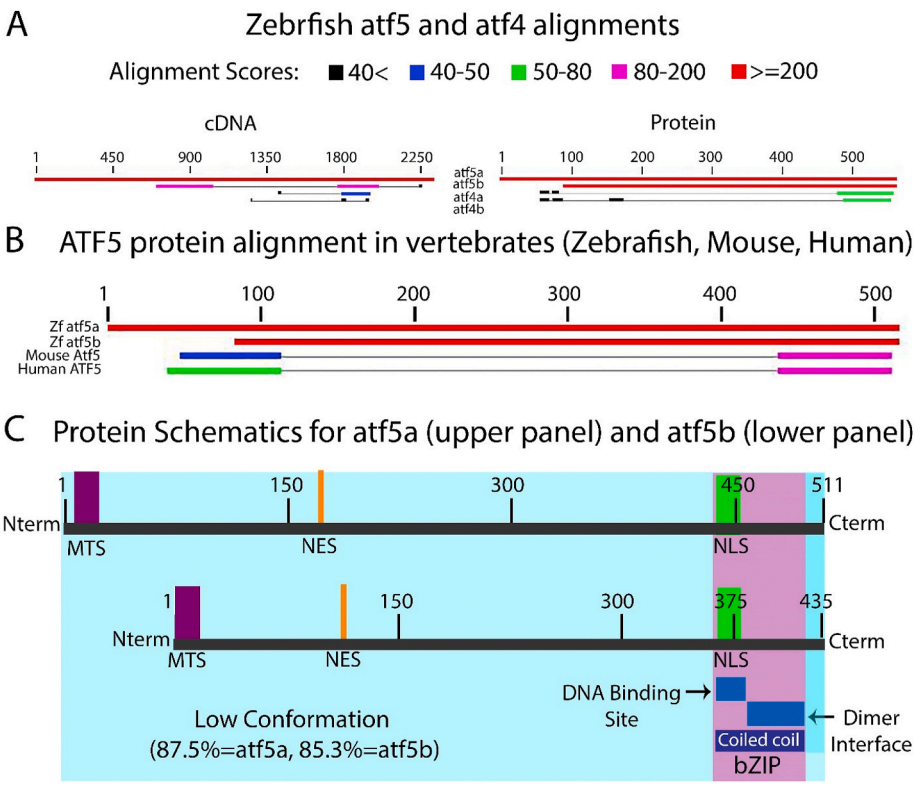

Fig. 1. Alignment and conservation of *atf5a* and *atf5b* gene products. (**A**) Alignments of *atf5a*, *atf5b*, *atf4a* and *atf4b* zebrafish cDNAs (left panel) and corresponding encoded proteins (right panel). (**B**) Protein alignment of human ATF5, mouseAtf5, and the two zebrafish paralogs atf5a and atf5b. (**C**) Schematic representation of putative 3D structures and signature domains of atf5a (top) and atf5b (bottom). A mitochondrial targeting sequence (MTS, purple) is indicated in the proximal Nterm of each paralog. A nuclear export signal (NES, orange) in the distal Nterm, a nuclear localization sequence (NSL, green) inside the highly conserved basic leucine zipper signature domain (bZIP) domain in the C-term (magenta) are depicted. Large central regions in both proteins (87.5% for atf5a and 85.3% of atf5b) were predicted low conformation.

(WISH) in larvae at different developmental stages. We assessed the embryonic expression in 6, 12 and 24hpf embryos (n = 30/gene/stage, Fig. 2). At 6hpf, the mid-epiboly embryos (Fig. 2A, dark brown) engulfed about ½ of the yolk sac (lighter beige). We found ubiquitous staining in the animal pole for *atf5a* (Fig. 2C) and for *atf5b* which appeared fainter (Fig. 2D). At 12hpf, we saw no distinguishable expression patterns for

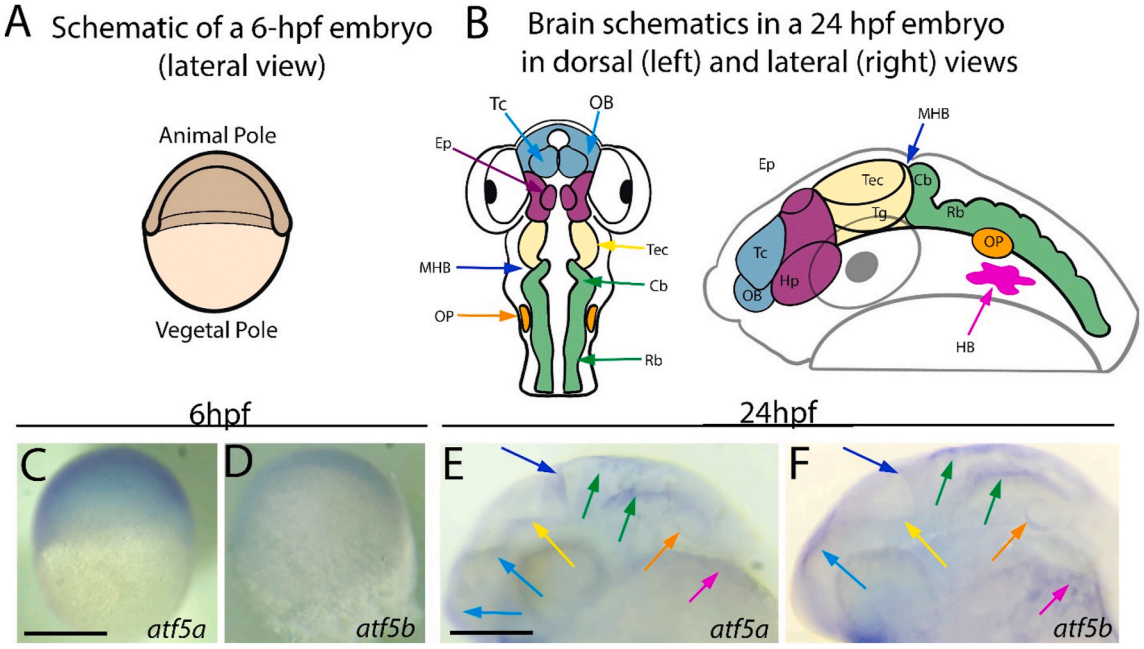

Fig. 2. Embryonic expression of the *atf5a* and *atf5b* genes. (**A**) Schematic lateral view (animal pole dorsal) of a mid-epiboly (~6hpf) zebrafish embryo (dark brown) engulfing the top half of the yolk sac (beige). (**B**) Schematics of the developing brain at 24hpf in a dorsal view (left, rostral to the top), and a lateral view (right, rostral to the left). The early brain subdivisions are distinguishable (Nishizawa and Nagata, 1992): forebrain (presumptive olfactory bulbs (OB) and telencephalon (Tc) in blue, and diencephalon in magenta) (Hai and Hartman, 2001), midbrain (presumptive tectum (Tec) and tegmentum (Tg) in yellow, and (Vinson et al., 2002) the hindbrain (presumptive cerebellum (Cb) and rhombencephalon (Rb) in green). The midbrain-hindbrain boundary (MHB, dark blue arrow) is also clearly visible as well as the otic placode (OP, orange), the hepatic bud (HB, pink) is also depicted. (**C** and **D**) Lateral views and of 6hpf embryos showing ubiquitous maternal expression of a*tf5a* (C) and *atf5b* (D). (**E** and **F**) Lateral views of 24hpf embryos showing a*tf5a* (E) and *atf5b* (F) gene expression in structures/regions highlighted by colored-coded arrows following the schematics in B. Scale bars: in C = 80 μm and in E = 100 μm.

either genes (not shown). At 24hpf, transparent embryos had defined external rostral features like eyes and olfactory placodes as well as distinguishable internal presumptive organs like the brain and the otic placodes (Fig. 2B). We found *atf5a* expression (Fig. 2E) in the developing brain, namely in the olfactory bulbs (OB, light blue arrows) of the forebrain, in the tectum (Tec, yellow arrow) of the midbrain, in the midbrain-hindbrain boundary (MHB, dark blue arrow), and in the hindbrain (green arrows). The *atf5a* gene was also expressed in the ventral part of the otic placode (OP, orange arrow) and in the liver primordium or hepatic bud (HB, pink arrow). For the *atf5b* gene (Fig. 2F), we found mostly the same expression pattern in the prementioned developing structures, for the exception in the forebrain, where it was absent from the OBs, but present instead in the rostral part of the telencephalon (light blue arrow). Thus, at this early stage most of *atf5a* and *atf5b* genes expression was overlapping.

2.3. 3: atf5a expression in the larva

Next, we monitored older larvae at 2, 3 and 5dpf with antisense (n = 30/stage) and sense (n = 5/stage) RNA probes against *atf5a* (Fig. 3). Most notably in whole larvae (3A) and at all observed stages we found that *atf5a* was expressed in the developing liver (black arrows), in the olfactory organs (B), in the inner ear (C) and in the midbrain and hindbrain (D). At all stages, both olfactory organs were strongly expressing *atf5a* (C, left column). At higher magnification, the olfactory epithelia (OE) displayed a salt and pepper appearance (B, right column) suggesting that only a subset of cells were expressing *atf5a*. In the sensory epithelia (SE) of the inner ear (C and white asterisk in D upper panel) *atf5a* gene expression seemed more uniform in all structures. Specifically, all cells of the maculae (orange asterisks in C: anterior macula (am) and posterior macula (pm) in top schematic), as well as of the three cristae (blue asterisks: anterior (ac), medial (mc) and posterior crista (pc) in top schematic) were expressing *atf5a*. However, the expression in SE seemed weaker in 5dpf larvae, suggesting a possible downregulation of this gene at later stages. Finally, in the brain (D), at 2dpf we noticed weak expression in the telencephalic olfactory bulbs (OBs) and a more intense expression at the midbrain-hindbrain (MHB) boundary. At later stages, and especially at 5dpf, the expression was much stronger in the OBs (pink asterisks), but also in the *tectum mesencephali* (yellow asterisks) and the metencephalic *medulla oblongata* (green asterisks). Interestingly all these regions remain neurogenic in adult Fish (Kaslin et al., 2008), raising the possibility that atf5a has a role in neuroprogenitors maintenance/proliferation similar to what was described in rodents.

2.4. 4: atf5b expression in the larva

Next, we monitored older larvae at 2, 3 and 5dpf with antisense (n = 30/stage) and sense (n = 5/stage) RNA probes against *atf5b* (Fig. 4). Most notably in whole larvae (A) and at all observed stages we found

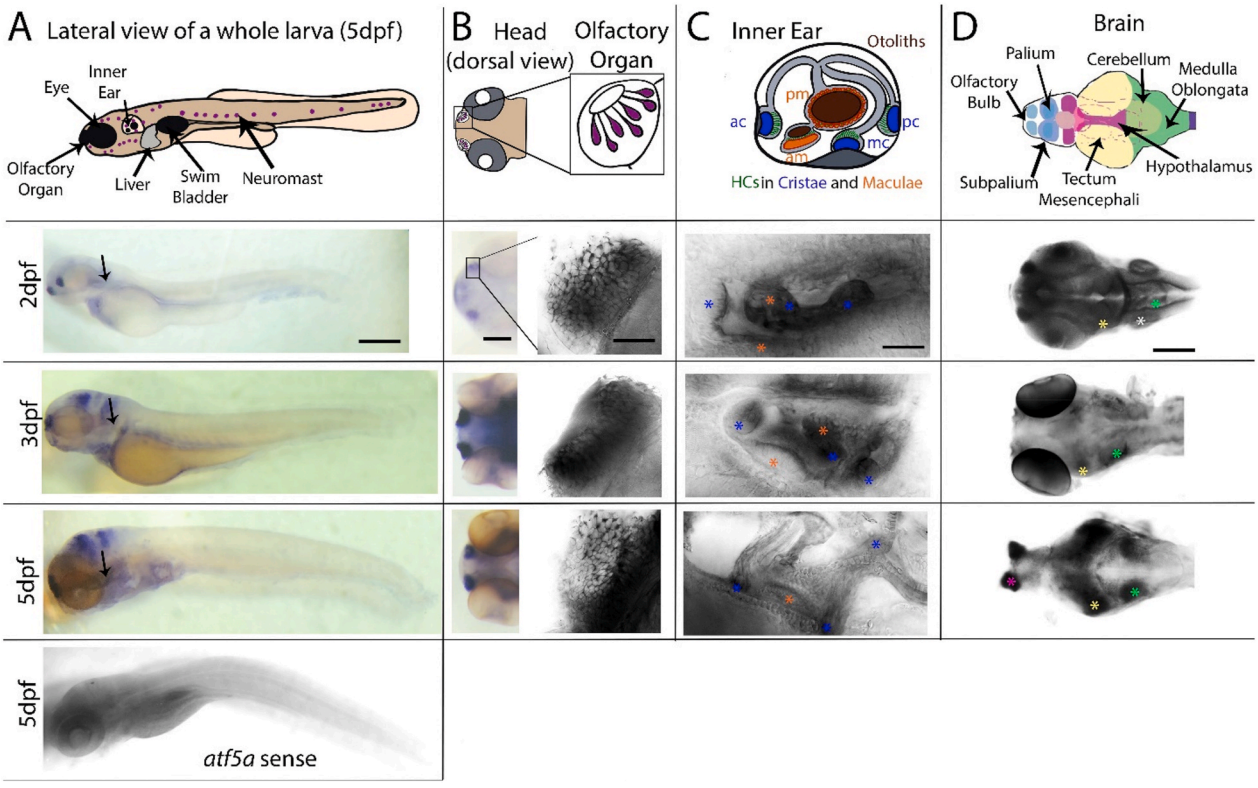

Fig. 3. Larval expression of *atf5a*. (**A**) Schematic of a whole larva at 5dpf (top panel) locating the major sensory organs (eyes, olfactory organs and neuromasts (NMs) of the superficial sensory lateral line organ, LL) as well as the swim bladder and the liver. Whole larvae were hybridized with an antisense RNA probe at 2, 3 and 5dpf (3 top panels) and with a sense probe at 5dpf (lower panel). Black arrows indicate the developing liver. (**B**) Dorsal views of the rostral part of the larva (left column) showing strong *atf5a* expression in the olfactory epithelia (OE) of olfactory organs. OE are shown at higher magnification (right column). (**C**) Lateral views of the inner ear (schematized in the top panel highlighting all sensory epithelia with hair cells (HCs, green): anterior (am) and posterior maculae (pm, orange) sitting underneath otoliths (brown), and anterior (ac), median (mc) and posterior cristae (pc, in blue) sitting at the end of each corresponding semicircular canal. The *atf5a* gene is expressed in maculae (orange asterisks) and cristae (blue asterisks) at all stages. (**D**) Dorsal views of the head showing the different brain regions. Schematic adapted from Torres-Hernandez et al. (2016) (top panel) depicting telencephalon (blue), diencephalon (magenta), mesencephalon (yellow) and metencephalon (green). At 2dpf and 3dpf (2nd and third panels) whole larva had visible *atf5a* expression in the inner ear (white asterisk), the *tecta mesencephali* (yellow asterisks), and the metencephalic *medulla oblongata* (green asterisks). At 5dpf, dissected brains showed strong expression in the sub-mentioned regions and in the olfactory bulbs (OBs, pink asterisks). Scale bars: in A = 200 μm, in B (left column) = 75 μm, in B (right column) = 25 μm, in C = 50 μm, and in D = 150 μm.

that *atf5b* was expressed in the developing liver (black or white arrows), in the superficial sensory organ called the lateral line (LL), which is formed by neuromasts (NMs), and in the inner ear (C). Cranial, trunk and tail NMs forming the anterior LL (aLL) and the posterior (LL) all displayed strong *atf5b* expression which we found in nascent and mature NMs. Furthermore, the expression did not appear restricted to a specific cell type but seemed present in all peripheral support cells as well as in central hair cells (HCs). In the inner ear, we detected a strong expression in all epithelial patches of the inner ear (C), namely in maculae (orange asterisks) and in cristae (blue asterisks), which also appeared to express *atf5b* in all cells of the sensory epithelia (SE), being support cells or HCs. Thus, *atf5b* was mostly expressed in the sensory epithelia of the inner ear and the evolutionary linked LL.

2.5. 5: atf5b expression in the lateral line organ (LL)

The NMs of the LL are evolutionarily linked to the SE of the inner ear with which they share numerous structural, ultrastructural, and gene expression similitudes Behra et al., 2012; Chiu et al., 2008; Denans et al., 2019; Dijkgraaf, 1964; Uribe et al., 2018. The NMs are sensory patches composed of 3 cell types with centrally located hair cells (HCs) that are surrounded by support cells comprising the most peripheral mantle cells. HCs are mechanoreceptors deflected by water currents in the LL and by sounds waves in the inner ear. In fish, all HCs can regenerate unlike HCs in postnatal mammals. Because of the experimental ease of access, the LL is extensively used to study HC regeneration and a subgroup of support cells are HC progenitors Thomas, 2014; Lush, 2014; Behra, 2009. To confirm the identity of cells that were expressing *atf5b* in NMs, we made use of an online freely available resource that was constructed from single cell RNA sequencing analyses (scRNA-seq) performed on cells purified from NMs of 5dpf larvae (https://piotrowskilab.shinyapps.io/neuromast_homeostasis_scrnaseq_2018/) (Lush et al., 2019). This interrogatable database substantially refined the cell constitution of NMs from the 3/4 originally described cell types to 14 different clusters of cells based on their respective transcriptome (Fig. 5A). This approach counted the actual number of transcripts/cell for any given gene, thus providing a quantitative complement to qualitative hybridization approaches. For the *atf5b* transcripts, we found that they were detected in all 14-cell cluster/types (purple dots in B) corroborating the *atf5b* expression patterns. The violin plot further reported how many *atf5b* transcripts (in an arbitrary unit = expression fold) were found per cluster (C). The *atf5b* transcripts seemed most abundant in cells clustering with peripheral mantle cells (cluster 6), non-dividing Anterior-Posterior (AP)-Pole support cells (cluster 13), and central support cells (cluster 7, 8 and 9) which all represent putative HC progenitors. Interestingly, *atf5b* transcripts were excluded from young HCs (cluster 2), poorly expressed in mature HCs (cluster 1) and differentiating HC progenitors (cluster 4). Taken together, this was suggesting that *atf5b* was predominantly expressed in HC progenitors and gradually turned off in HCs, suggesting a role for atf5b in maintenance of HC progenitors, reminiscent of the role described in neuroprogenitors in rodent brains (Angelastro et al., 2003, 2005; Lee et al., 2012; Mason et al., 2005).

3. Discussion

We described the temporal and spatial dynamic of the expression pattern of *atf5a* and *atf5b* paralogous genes during embryonic and larval development in zebrafish. Both genes were expressed early but it remains unclear what early function they perform or if either gene could

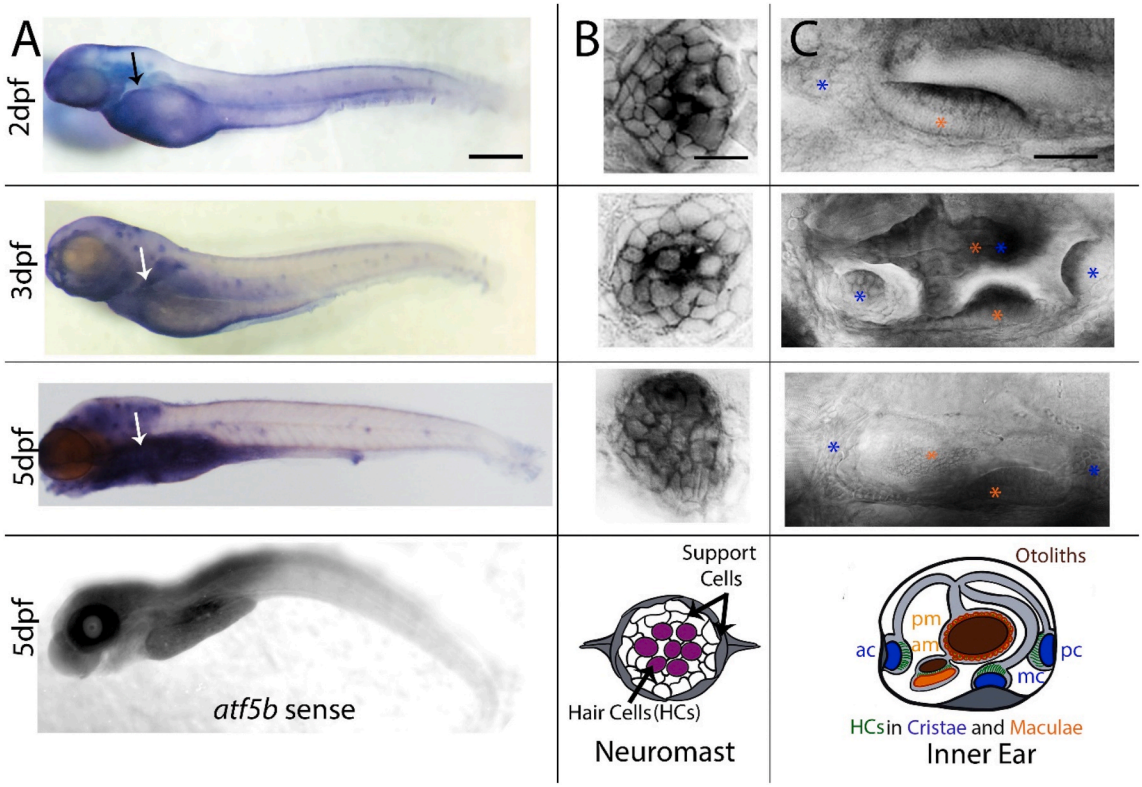

Fig. 4. Larval expression of *atf5b*. (**A**) Whole larva at 2, 3 and 5dpf hybridized with an antisense RNA probe against the *atf5b* gene (3 top panels) and a sense probe (last panel). Black and white arrows indicate the developing liver. (**B**) High magnification of neuromasts (NMs) in 2, 3 and 5dpf larvae (top panels), which are schematized (bottom panel) with centrally located hair cells HCs (magenta) surrounded by two type of support cells (white and grey). (**C**) lateral views of the inner ear (schematized in bottom panel) of a 2, 3 and 5dpf larva (top panels), showing strong *atf5b* expression in the sensory patches of the inner ear, namely in the anterior (ac), median (mc) and posterior (pc) cristae (blue asterisks) as well as the anterior (am) and posterior (pm) maculae (orange asterisks). Scale bars: in A = 200 μm, in B = 40 μm, and in C = 75 μm.

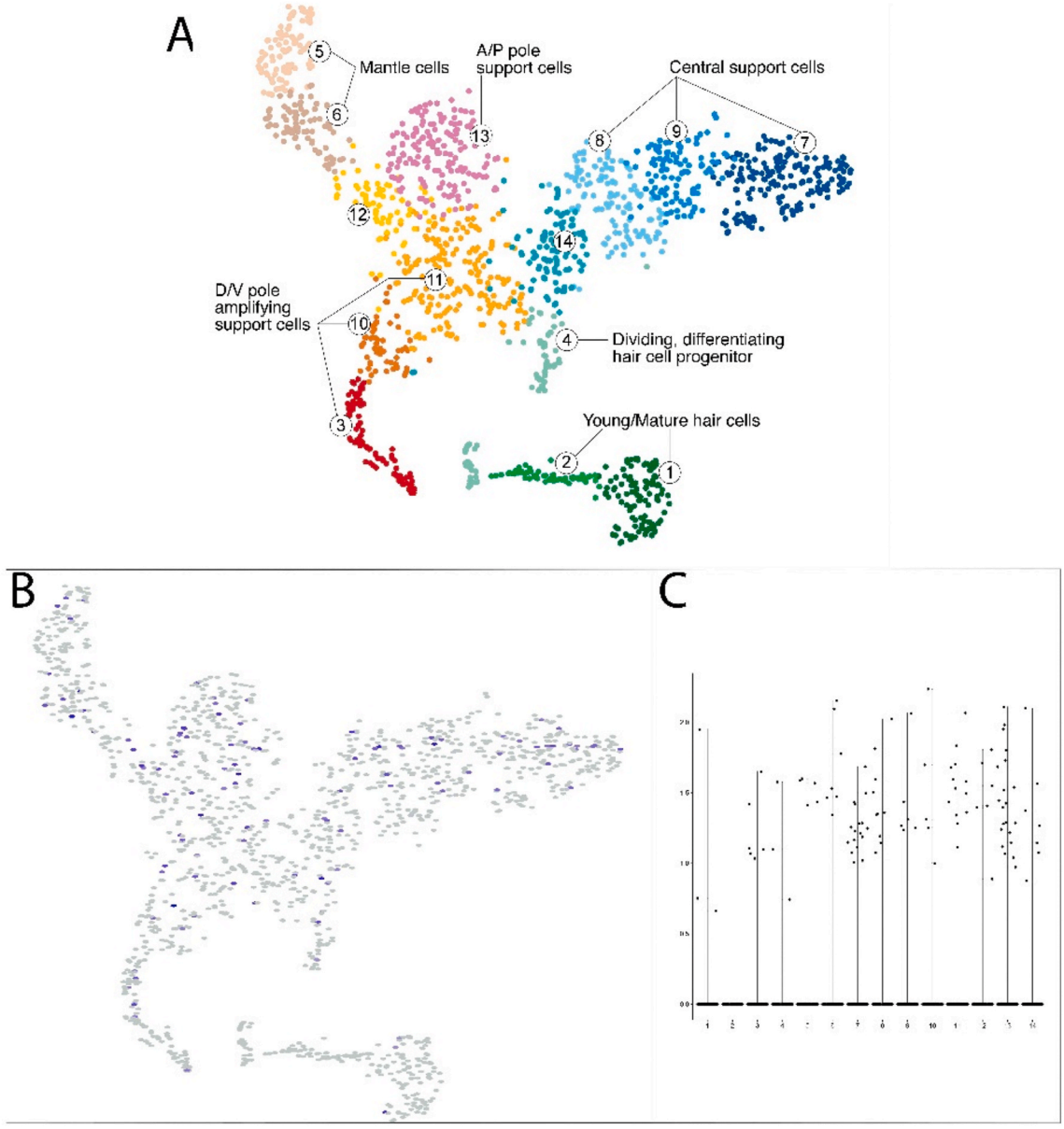

Fig. 5. scRNA-Seq analyses corroborate expression of *atf5b* in NMs. (**A**) Overall representation in a t-distributed Stochastic Neighbor Embedding (t-SNE) plot of 14 cell clusters based on mRNA expression profiles established from 1521 purified cells from NMs of 5dpf larvae. (**B**) t-SNE plot showing specifically the *atf5b* expressing cells (purple). (C) Violin plot showing in the X axis the cluster identity (1–14) to which the atf5b expressing cells belong, and the Y axis the *atf5b* expression fold (0–2 arbitrary unit, AU). Most *atf5b* expressing cells cluster in 6 (mantle cells), 7, 8 and 9 (central support cells) and in 13 (AP non-dividing support cells).

compensate for the absence of the other. Double-KOs will answer these questions. A number of cellular functions have been proposed in cell systems, like the cellular stress response which is happening mostly at the translational level, when ATF5 is up-regulated in response to various stressors (Zhou et al., 2008), including amino acid limitation (Watatani et al., 2007), arsenide exposure (Watatani et al., 2008), and classical endoplasmic reticulum (ER) stressors (Hatano et al., 2013). The translational up-regulation of ATF5 under stress condition is mediated by phosphorylation of eukaryotic initiation factor 2α (eIF2α), (Watatani et al., 2008). This could be an early defense mechanism present in the embryo which could be studied in wild type and mutant background, and if either KOs is adult viable, the respective maternal contribution could be assessed.

At 24hpf we found strong expression in the brain for both *atf5a* and *atf5b* genes that was mostly overlapping in the midbrain and hindbrain, but not in the forebrain where each gene was expressed in different regions, suggesting at least partial non-redundant functions. It will be interesting to identify the expressing cells and possibly correlate them to previously documented progenitor pools (Stigloher et al., 2008). Later, at 3 and at 5dpf, we mostly found only *atf5a* expression in the olfactory bulbs, the *tectum mesencephali* and the *medulla oblongata*. Interestingly, all of those regions are documented neurogenic areas in the embryo and the adult fish ((Kermen et al., 2013) (Kaslin et al., 2008) (Schmidt et al., 2013)), suggesting that atf5a could have a role in maintenance of neuroprogenitors cells paralleling the finding from rodent brains (Angelastro et al., 2003, 2005; Lee et al., 2012; Mason et al., 2005). Alternatively, the *atf5*a brain expression especially in later larval stages might correspond to mature neuronal populations, which was also previously described in developing and adult mouse brains (Torres--Peraza et al., 2013). They further showed that the basal expression of *Atf5* could be increased by ER stressors and proposed that Atf5 was part of the neuronal endoplasmic reticulum stress response protecting neurons from apoptosis (Torres-Peraza et al., 2013). This raises the interesting possibility of atf5a acting as a neuroprotector (Sears and

Angelastro, 2017; Angelastro, 2017; Cates et al., 2016; Chen et al., 2012; Dluzen et al., 2011; Karpel-Massler et al., 2016; Monaco et al., 2007) which could be assessed in the context of the whole animal.

The liver primordium was expressing both *atf5a* and *atf5b* genes from 24hpf onwards, weakly at first but with the expression becoming stronger overtime, especially for *atf5b*. At 2dpf, the liver bud becomes more prominent extending from the midline to the yolk, lying just anterior to the presumptive swim bladder and around 3dpf, hepatocyte differentiation and hepatic outgrowth are rapidly amplifying (Ober et al., 2003; Field et al., 2003) (Chu and Sadler, 2009). The gradually stronger expression of *atf5b* seemed to parallel the development and maturation of the liver which becomes functional ~5dpf, when the yolk sack reserves are depleted, and the larva must sustain itself by ingesting and digesting food. It is tempting to speculate that one or both paralogs are involved in hepatocyte differentiation and maturation as demonstrated in cell lines (Nakamori et al., 2016, 2017). Alternatively either or both paralogs could be implicated in the stress response of mature hepatocytes which was also previously demonstrated (Pascual et al., 2008), which again could be assessed in wild type and mutant backgrounds in the physiological context of whole animals.

From 2dpf onward, both *atf5a* and *atf5b* genes were apparently co-expressed in all cells of the sensory epithelia (SE) in the inner ear, with *atf5b* getting stronger and *atf5a* weaker in later developmental stages. *Atf5* expression in the inner ear has not been reported previously to our knowledge, and it will be important to probe the respective role of each paralogs using double-KO animals specifically. It is tempting to hypothesize an early interchangeable role at least during the development of the SE, and a possible later specialization for each paralog, when the SE is fully formed but regenerate HCs on demand. Interestingly, when looking at the LL, which is structurally, physiologically, and evolutionary closely linked to the inner ear (Denans et al., 2019; Uribe et al., 2018; Behra et al., 2012; Chiu et al., 2008; Dijkgraaf, 1964), we exclusively found *atf5b* expression. This was confirmed by using the available single-cell RNA seq online database (Lush et al., 2019), showing no expression of *atf5a*. This tool also allowed to refine the expression of *atf5b* and suggested that it was weaker or even absent in some HCs and significantly stronger in support cells, and mantle cells. Notably, it was expressed in cell clusters that might represent stem cells of the NMs due to expression of several stem cells markers (Seleit et al., 2017; Steiner et al., 2014), suggesting a possible role during HC regeneration for atf5, which will be interesting to explore.

Finally, we found strong and exclusive *atf5a* expression in the olfactory epithelium (OE) that was paralleling prior findings in rodents, suggesting that Atf5 was necessary for OSNs maturation and maintenance (Wang et al., 2012) (Nakano et al., 2016). Fish, lack the vomeronasal organ (VNO) and epithelium (VNE) that is specialized in pheromone detection, but instead perform all olfactory functions via one single OE (Sato et al., 2005) (Saraiva et al., 2015). The ciliated OSNs are thought to detect the volatile odorants while the microvillous OSNs are thought to detect pheromones, thus exerting the role of OSNs found in the VNO (Hansen and Zeiske, 1993) (Hansen and Zielinski, 2005) (Sato et al., 2005). Immature OSNs express up to 1000 different olfactory receptors (ORs) and part of the maturation process consist in committing to a single one for the remaining of the OSN life. A recent and very elegant study demonstrated that Atf5 was part of the intricate mechanism presiding the choice of a specific OR during OSNs maturation (Dalton et al., 2013). It remains to be demonstrated if the same exquisite ATF5-dependent final differentiation is taking place in fish OSNs. Our work provides an evolutionary insight into the expression pattern of *Atf5* during development, as well as a stepping stone for future functional analyses. Taking advantages of what this vertebrate model has to offer, the role of Atf5 can be addressed in an organ specific manner in the physiological context of a whole animal.

4. Experimental procedures

4.1. Fish husbandry

We performed animal care and husbandry following previously published protocols (Press.teohe zebr, 2000) and NIH guidelines with authorization by IACUC protocol #A880110. Adult zebrafish were maintained in 5 or 10 L tanks in a semi-closed and automated system (Techniplast). Embryos and larvae from inbred wild type (genetic background = TAB-5 = Tub x AB) were used for all experiments, while performing all developmental staging according to Kimmel et al. (1995).

4.2. Whole-mount in-situ hybridization (WISH)

We performed Trizol (Invitrogen) extraction of total RNAs from 5dpf larvae to synthetize sense and antisense RNA probes. Using the Super-Script III One-Step retro-transcription kit (Sigma 12574-026) to retro-transcribe both genes, we designed the following gene specific primers (GSPs) for *atf5a* (Forward: CAAACTGGGCAAATGCGACA, and Reverse: TTCGCTGGGTTCTGTCTTCC) and for *atf5b* (Forward: TGCA-TATTTCAACCGCGCAC and Reverse: GGTGGGATTGAGGAACCAGG) with T7 (atgctaatacgactcactatagggaga) and T3 (atgcattaaccctcac-taaaggga) promoter sequences attached to the forward and reverse primers, respectively. The expected amplicon length was 667bp for *atf5a* and 665bp for *atf5b*. Next, we performed WISH as described previously with minor modifications (Thisse and Thisse, 2014). First, embryos were dechorionated and rehydrated in methanol/10X PBS gradient solutions (75% methanol, 50% methanol, 25% methanol) for 5 min and then rinsed in PBST (1%Tween 20) for 5 min. Animals older than 24hpf were bleached with 30% H2O2 (Sigma) for approximately 20 min, followed by enzymatic digestion of larva older than 2dpf with 2 mg/ml of Proteinase K (Ambion) for 7 min. Fixation was performed at room temperature (RT) (4% paraformaldehyde) for 45 min. After rinsing 5 × 5min in Blocking Buffer for WISH (1X PBS, 0.1% Tween 20, 0.1% BSA, 1% DMSO), we pre-hybridized larvae in hybridization mix (HM) (50% Formamide, 5X SSC, 1 mg/mL Yeast RNA, 50 μm/mL Heparin, 0.1% Tween 20, 5 mM EDTA, 9 mM Citric Acid in DEPC treated water) for 4–6 h. Next, all specimens were hybridized with the pre-heated probe (final concentration = 1 ng/μl) overnight at 65 °C. We washed larvae in a series of HM solutions in 2X SSC (75%, 50%, 25%) for 10 min each, followed by two 30-min washes of 0.2X SSC, all at 65 °C. Next, animals were rinsed in 0.2X SSC gradient solutions in PBST (75%, 50%, 25%) for 10 min each at RT. We pre-incubated all specimens in Blocking Buffer for 4–6 h and then incubated in pre-absorbed anti-DIG-AB against fish powder in blocking buffer (1/3000) overnight (O/N). Finally, we rinsed all animals in PBST 6 × 15 min followed by two 5-min washes in Alkaline Phosphatase Buffer (APB) (100 mM Tris pH9.5, 50 mM MgCl2, 100 mM NaCl, 0.1% Tween 20, levamisole), followed by revelation using BM Purple (100%) in the dark.

4.3. Image acquisition

We acquired Images on an inverted Axiovert (Zeiss) with Axiovision and post-processed as needed with the Zen Lite 2.6 software. Final figures were created with Adobe Photoshop and Illustrator.

Funding sources

This work was supported by grants from the National Science Foundation NSF (PRCEN-CREST-II # 1736019) to MB and from the National Institute of Health (NIGMS-RISE #R25GM061838) to RRM.

Declaration of competing interest

None.

Acknowledgements

We acknowledge for husbandry and general bench work the fish-room technician: Neidibel Martínez and the undergraduate students: Tiffany Tossas, Lorianie Colóm, Keisy Bonano, Kenny Colón and Alysa Alejandro.

Appendix A. Supplementary data

Supplementary data to this article can be found online at https://doi.org/10.1016/j.gep.2020.119126.

References

Al Sarraj, J., Vinson, C., Thiel, G., 2005. Regulation of asparagine synthetase gene transcription by the basic region leucine zipper transcription factors ATF5 and CHOP. Biol. Chem. 386 (9), 873–879.
Angelastro, J.M., 2017. Targeting ATF5 in cancer. Trends Cancer 3 (7), 471–474.
Angelastro, J.M., Ignatova, T.N., Kukekov, V.G., Steindler, D.A., Stengren, G.B., Mendelsohn, C., et al., 2003. Regulated expression of ATF5 is required for the progression of neural progenitor cells to neurons. J. Neurosci. 23 (11), 4590–4600.
Angelastro, J.M., Mason, J.L., Ignatova, T.N., Kukekov, V.G., Stengren, G.B., Goldman, J. E., et al., 2005. Downregulation of activating transcription factor 5 is required for differentiation of neural progenitor cells into astrocytes. J. Neurosci. 25 (15), 3889–3899.
Arias, A., Lame, M.W., Santarelli, L., Hen, R., Greene, L.A., Angelastro, J.M., 2012. Regulated ATF5 loss-of-function in adult mice blocks formation and causes regression/eradication of gliomas. Oncogene 31 (6), 739–751.
Behra, M, et al., 2009. Phoenix Is Required for Mechanosensory Hair Cell Regeneration in the Zebrafish Lateral Line. PloS Genetics.
Behra, M., Gallardo, V.E., Bradsher, J., Torrado, A., Elkahloun, A., Idol, J., et al., 2012. Transcriptional signature of accessory cells in the lateral line, using the Tnk1bp1: EGFP transgenic zebrafish line. BMC Dev. Biol. 12, 6.
Cates, C.C., Arias, A.D., Nakayama Wong, L.S., Lame, M.W., Sidorov, M., Cayanan, G., et al., 2016. Regression/eradication of gliomas in mice by a systemically-deliverable ATF5 dominant-negative peptide. Oncotarget 7 (11), 12718–12730.
Chen, A., Qian, D., Wang, B., Hu, M., Lu, J., Qi, Y., et al., 2012. ATF5 is overexpressed in epithelial ovarian carcinomas and interference with its function increases apoptosis through the downregulation of Bcl-2 in SKOV-3 cells. Int. J. Gynecol. Pathol. 31 (6), 532–537.
Chiu, L.L., Cunningham, L.L., Raible, D.W., Rubel, E.W., Ou, H.C., 2008. Using the zebrafish lateral line to screen for ototoxicity. J. Assoc. Res. Otolaryngol 9 (2), 178–190.
Chu, J., Sadler, K.C., 2009. New school in liver development: lessons from zebrafish. Hepatology 50 (5), 1656–1663.
Dalton, R.P., Lyons, D.B., Lomvardas, S., 2013. Co-opting the unfolded protein response to elicit olfactory receptor feedback. Cell 155 (2), 321–332.
Denans, N., Baek, S., Piotrowski, T., 2019. Comparing sensory organs to define the path for hair cell regeneration. Annu. Rev. Cell Dev. Biol. 35, 567–589.
Dijkgraaf, S., 1964. The supposed use of the lateral line as an organ of hearing in fish. Experientia 20 (10), 586–587.
Dluzen, D., Li, G., Tacelosky, D., Moreau, M., Liu, D.X., 2011. BCL-2 is a downstream target of ATF5 that mediates the prosurvival function of ATF5 in a cell type-dependent manner. J. Biol. Chem. 286 (9), 7705–7713.
Field, H.A., Ober, E.A., Roeser, T., Stainier, D.Y., 2003. Formation of the digestive system in zebrafish. I. Liver morphogenesis. Dev. Biol. 253 (2), 279–290.
Fiorese, C.J., Schulz, A.M., Lin, Y.F., Rosin, N., Pellegrino, M.W., Haynes, C.M., 2016. The transcription factor ATF5 mediates a mammalian mitochondrial UPR. Curr. Biol. 26 (15), 2037–2043.
Fukasawa, Y., Tsuji, J., Fu, S.C., Tomii, K., Horton, P., Imai, K., 2015. MitoFates: improved prediction of mitochondrial targeting sequences and their cleavage sites. Mol. Cell. Proteomics 14 (4), 1113–1126.
Glasauer, S.M., Neuhauss, S.C., 2014. Whole-genome duplication in teleost fishes and its evolutionary consequences. Mol. Genet. Genom. 289 (6), 1045–1060.
Greene, L.A., Lee, H.Y., Angelastro, J.M., 2009. The transcription factor ATF5: role in neurodevelopment and neural tumors. J. Neurochem. 108 (1), 11–22.
Hai, T., Hartman, M.G., 2001. The molecular biology and nomenclature of the activating transcription factor/cAMP responsive element binding family of transcription factors: activating transcription factor proteins and homeostasis. Gene 273 (1), 1–11.
Hansen, A., Zeiske, E., 1993. Development of the olfactory organ in the zebrafish, Brachydanio rerio. J. Comp. Neurol. 333 (2), 289–300.
Hansen, A., Zielinski, B.S., 2005. Diversity in the olfactory epithelium of bony fishes: development, lamellar arrangement, sensory neuron cell types and transduction components. J. Neurocytol. 34 (3–5), 183–208.
Hansen, M.B., Mitchelmore, C., Kjaerulff, K.M., Rasmussen, T.E., Pedersen, K.M., Jensen, N.A., 2002. Mouse Atf5: molecular cloning of two novel mRNAs, genomic organization, and odorant sensory neuron localization. Genomics 80 (3), 344–350.
Hatano, M., Umemura, M., Kimura, N., Yamazaki, T., Takeda, H., Nakano, H., et al., 2013. The 5'-untranslated region regulates ATF5 mRNA stability via nonsense-mediated mRNA decay in response to environmental stress. FEBS J. 280 (18), 4693–4707.
Karpel-Massler, G., Horst, B.A., Shu, C., Chau, L., Tsujiuchi, T., Bruce, J.N., et al., 2016. A synthetic cell-penetrating dominant-negative ATF5 peptide exerts anticancer activity against a broad spectrum of treatment-resistant cancers. Clin. Canc. Res. 22 (18), 4698–4711.
Kaslin, J., Ganz, J., Brand, M., 2008. Proliferation, neurogenesis and regeneration in the non-mammalian vertebrate brain. Philos. Trans. R. Soc. Lond. B Biol. Sci. 363 (1489), 101–122.
Kermen, F., Franco, L.M., Wyatt, C., Yaksi, E., 2013. Neural circuits mediating olfactory-driven behavior in fish. Front. Neural Circ. 7, 62.
Kimmel, C.B., Ballard, W.W., Kimmel, S.R., Ullmann, B., Schilling, T.F., 1995. Stages of embryonic development of the zebrafish. Dev. Dynam. 203 (3), 253–310.
la Cour, T., Kiemer, L., Molgaard, A., Gupta, R., Skriver, K., Brunak, S., 2004. Analysis and prediction of leucine-rich nuclear export signals. Protein Eng. Des. Sel. 17 (6), 527–536.
Lee, H.Y., Angelastro, J.M., Kenney, A.M., Mason, C.A., Greene, L.A., 2012. Reciprocal actions of ATF5 and Shh in proliferation of cerebellar granule neuron progenitor cells. Dev Neurobiol 72 (6), 789–804.
Lush, ME, et al., 2014. Sensory Hair Cell Regeneration in the Zebrafish Lateral Line. Dev. Dyn.
Lush, M.E., Diaz, D.C., Koenecke, N., Baek, S., Boldt, H., St Peter, M.K., et al., 2019. scRNA-Seq reveals distinct stem cell populations that drive hair cell regeneration after loss of Fgf and Notch signaling. Elife 8.
Mason, J.L., Angelastro, J.M., Ignatova, T.N., Kukekov, V.G., Lin, G., Greene, L.A., et al., 2005. ATF5 regulates the proliferation and differentiation of oligodendrocytes. Mol. Cell. Neurosci. 29 (3), 372–380.
Monaco, S.E., Angelastro, J.M., Szabolcs, M., Greene, L.A., 2007. The transcription factor ATF5 is widely expressed in carcinomas, and interference with its function selectively kills neoplastic, but not nontransformed, breast cell lines. Int. J. Canc. 120 (9), 1883–1890.
Nakamori, D., Takayama, K., Nagamoto, Y., Mitani, S., Sakurai, F., Tachibana, M., et al., 2016. Hepatic maturation of human iPS cell-derived hepatocyte-like cells by ATF5, c/EBPalpha, and PROX1 transduction. Biochem. Biophys. Res. Commun. 469 (3), 424–429.
Nakamori, D., Akamine, H., Takayama, K., Sakurai, F., Mizuguchi, H., 2017. Direct conversion of human fibroblasts into hepatocyte-like cells by ATF5, PROX1, FOXA2, FOXA3, and HNF4A transduction. Sci. Rep. 7 (1), 16675.
Nakano, H., Iida, Y., Suzuki, M., Aoki, M., Umemura, M., Takahashi, S., et al., 2016. Activating transcription factor 5 (ATF5) is essential for the maturation and survival of mouse basal vomeronasal sensory neurons. Cell Tissue Res. 363 (3), 621–633.
Nguyen, Ba AN., Pogoutse, A., Provart, N., Moses, A.M., 2009. NLStradamus: a simple Hidden Markov Model for nuclear localization signal prediction. BMC Bioinf. 10, 202.
Nishizawa, M., Nagata, S., 1992. cDNA clones encoding leucine-zipper proteins which interact with G-CSF gene promoter element 1-binding protein. FEBS Lett. 299 (1), 36–38.
Ober, E.A., Field, H.A., Stainier, D.Y., 2003. From endoderm formation to liver and pancreas development in zebrafish. Mech. Dev. 120 (1), 5–18.
Pascual, M., Gomez-Lechon, M.J., Castell, J.V., Jover, R., 2008. ATF5 is a highly abundant liver-enriched transcription factor that cooperates with constitutive androstane receptor in the transactivation of CYP2B6: implications in hepatic stress responses. Drug Metab. Dispos. 36 (6), 1063–1072.
Persengiev, S.P., Green, M.R., 2003. The role of ATF/CREB family members in cell growth, survival and apoptosis. Apoptosis 8 (3), 225–228.
Persengiev, S.P., Devireddy, L.R., Green, M.R., 2002. Inhibition of apoptosis by ATFx: a novel role for a member of the ATF/CREB family of mammalian bZIP transcription factors. Genes Dev. 16 (14), 1806–1814.
Press. WMteEUoO, 2000. The Zebrafish Book: a Guide to the Laboratory Use of the Zebrafish (Danio Rerio), fourth ed. University of Oregon Press, Eugene.
Sampath, P., Pritchard, D.K., Pabon, L., Reinecke, H., Schwartz, S.M., Morris, D.R., et al., 2008. A hierarchical network controls protein translation during murine embryonic stem cell self-renewal and differentiation. Cell Stem Cell 2 (5), 448–460.
Saraiva, L.R., Ahuja, G., Ivandic, I., Syed, A.S., Marioni, J.C., Korsching, S.I., et al., 2015. Molecular and neuronal homology between the olfactory systems of zebrafish and mouse. Sci. Rep. 5, 11487.
Sato, Y., Miyasaka, N., Yoshihara, Y., 2005. Mutually exclusive glomerular innervation by two distinct types of olfactory sensory neurons revealed in transgenic zebrafish. J. Neurosci. 25 (20), 4889–4897.
Schmidt, R., Strahle, U., Scholpp, S., 2013. Neurogenesis in zebrafish - from embryo to adult. Neural Dev. 8, 3.
Sears, T.K., Angelastro, J.M., 2017. The transcription factor ATF5: role in cellular differentiation, stress responses, and cancer. Oncotarget 8 (48), 84595–84609.
Seleit, A., Kramer, I., Riebesehl, B.F., Ambrosio, E.M., Stolper, J.S., Lischik, C.Q., et al., 2017. Neural stem cells induce the formation of their physical niche during organogenesis. Elife 6.
Shinomura, T., Ito, K., Kimura, J.H., Hook, M., 2006. Screening for genes preferentially expressed in the early phase of chondrogenesis. Biochem. Biophys. Res. Commun. 341 (1), 167–174.
Steiner, A.B., Kim, T., Cabot, V., Hudspeth, A.J., 2014. Dynamic gene expression by putative hair-cell progenitors during regeneration in the zebrafish lateral line. Proc. Natl. Acad. Sci. U. S. A. 111 (14), E1393–E1401.
Stigloher, C., Chapouton, P., Adolf, B., Bally-Cuif, L., 2008. Identification of neural progenitor pools by E(Spl) factors in the embryonic and adult brain. Brain Res. Bull. 75 (2–4), 266–273.
Thisse, B., Thisse, C., 2014. In situ hybridization on whole-mount zebrafish embryos and young larvae. Methods Mol. Biol. 1211, 53–67.

Thomas, ED, et al., 2014. There and Back Again: Development and Regeneration of the Zebrafish Lateral Line System. Wiley Interdiscip Rev Dev Biol.
Torres-Hernandez, B.A., Colon, L.R., Rosa-Falero, C., Torrado, A., Miscalichi, N., Ortiz, J. G., et al., 2016. Reversal of pentylenetetrazole-altered swimming and neural activity-regulated gene expression in zebrafish larvae by valproic acid and valerian extract. Psychopharmacology (Berl) 233 (13), 2533–2547.
Torres-Peraza, J.F., Engel, T., Martin-Ibanez, R., Sanz-Rodriguez, A., Fernandez-Fernandez, M.R., Esgleas, M., et al., 2013. Protective neuronal induction of ATF5 in endoplasmic reticulum stress induced by status epilepticus. Brain 136 (Pt 4), 1161–1176.
Umemura, M., Tsunematsu, K., Shimizu, Y.I., Nakano, H., Takahashi, S., Higashiura, Y., et al., 2015. Activating transcription factor 5 is required for mouse olfactory bulb development via interneuron. Biosci. Biotechnol. Biochem. 79 (7), 1082–1089.
Umemura, M., Ogura, T., Matsuzaki, A., Nakano, H., Takao, K., Miyakawa, T., et al., 2017. Comprehensive behavioral analysis of activating transcription factor 5-deficient mice. Front. Behav. Neurosci. 11, 125.
Uribe, P.M., Villapando, B.K., Lawton, K.J., Fang, Z., Gritsenko, D., Bhandiwad, A., et al., 2018. Larval zebrafish lateral line as a model for acoustic trauma. eNeuro 5 (4).
Vinson, C., Myakishev, M., Acharya, A., Mir, A.A., Moll, J.R., Bonovich, M., 2002. Classification of human B-ZIP proteins based on dimerization properties. Mol. Cell Biol. 22 (18), 6321–6335.
Wang, H., Lin, G., Zhang, Z., 2007. ATF5 promotes cell survival through transcriptional activation of Hsp27 in H9c2 cells. Cell Biol. Int. 31 (11), 1309–1315.
Wang, S.Z., Ou, J., Zhu, L.J., Green, M.R., 2012. Transcription factor ATF5 is required for terminal differentiation and survival of olfactory sensory neurons. Proc. Natl. Acad. Sci. U. S. A. 109 (45), 18589–18594.
Watatani, Y., Kimura, N., Shimizu, Y.I., Akiyama, I., Tonaki, D., Hirose, H., et al., 2007. Amino acid limitation induces expression of ATF5 mRNA at the post-transcriptional level. Life Sci. 80 (9), 879–885.
Watatani, Y., Ichikawa, K., Nakanishi, N., Fujimoto, M., Takeda, H., Kimura, N., et al., 2008. Stress-induced translation of ATF5 mRNA is regulated by the 5'-untranslated region. J. Biol. Chem. 283 (5), 2543–2553.
Zhou, D., Palam, L.R., Jiang, L., Narasimhan, J., Staschke, K.A., Wek, R.C., 2008. Phosphorylation of eIF2 directs ATF5 translational control in response to diverse stress conditions. J. Biol. Chem. 283 (11), 7064–7073.